

Real-time, rapidly updating severe weather products for virtual globes

Travis M. Smith^a and Valliappa Lakshmanan^b

^aCorresponding Author

University of Oklahoma / Cooperative Institute of Mesoscale Meteorological Studies, and
National Oceanic and Atmospheric Administration / National Severe Storms Laboratory
120 David L. Boren Blvd., Norman, OK 73069
Tel: 405-325-6384 Fax: 405-325-6780
Email: Travis.Smith@noaa.gov

^bUniversity of Oklahoma / Cooperative Institute of Mesoscale Meteorological Studies, and
National Oceanic and Atmospheric Administration / National Severe Storms Laboratory
120 David L. Boren Blvd., Norman, OK 73069
Tel: 405-325-6384 Fax: 405-325-6780
Email: Valliappa.Lakshmanan@noaa.gov

ABSTRACT

It is critical that weather forecasters are able to put severe weather information from a variety of observational and modeling platforms into a geographic context so that warning information can be effectively conveyed to the public, emergency managers, and disaster response teams. The availability of standards for the specification and transport of virtual globe data products has made it possible to generate spatially precise, geo-referenced images and to distribute these centrally-created products via a web server to a wide audience.

In this paper, we describe the data and methods for enabling severe weather threat analysis information inside a KML framework. The method of creating severe weather diagnosis products that are generated and translating them to KML and image files is described. We illustrate some of the practical applications of these data when they are integrated into a virtual globe display. The availability of standards for interoperable virtual globe clients has not completely alleviated the need for custom solutions. We conclude by pointing out several of the limitations of the general-purpose virtual globe clients currently available.

Keywords: virtual globes; KML; weather; radar; tornadoes; hail

1 **1. Virtual globes in severe weather forecasting**

2
3 A critical role for weather forecasters is to warn of impending severe weather. In the United
4 States, this is accomplished by examining various observed and modeled datasets in real-time.
5 The most critical is Doppler radar, but satellite data, numerical models and surface observations
6 also play a key part. As the number and characteristics of these platforms increase, it has become
7 nearly impossible for a human forecaster to stay abreast of constantly arriving data. Hence,
8 severe weather algorithms have been devised to extract key information from these datasets in
9 real-time so as to provide heads-up guidance to forecasters. These severe weather products have
10 also been found useful in non-real-time mode in order to conduct post-event surveys and
11 research studies. Because a number of industries, such as transportation and electric utilities, can
12 take mitigating action on impending severe weather, severe weather diagnosis products are
13 useful beyond just weather forecasters.

14
15 Weather data comes in different spatial and temporal resolutions and in different native
16 coordinate systems. For example, the Doppler radar data used operationally are collected by a
17 rotating instrument placed on the earth's surface. A spherical volume of data is collected every
18 4-10 minutes (depending on atmospheric conditions) in a "plan" spatial resolution of
19 approximately 0.25km X 0.5 degrees. Geostationary satellites provide full disk scans of the
20 atmosphere once every 15-30 minutes with a spatial resolution of approximately 1-4 km. The
21 data are in a "satellite" projection that has to do with their angle of view from space. Surface
22 observations, meanwhile, are collected in an unsynchronized manner at numerous weather
23 stations located all over the country. All these datasets need to be visualized and analyzed by a

24 severe weather forecaster. It is very important to enable weather forecasters to put severe
25 weather information into a geographic context so that warning information can be effectively
26 conveyed to the public, emergency managers, and disaster response teams. Hence, virtual globe
27 software has been employed since the late 1990s as a data visualization system to assist
28 forecasters with mentally assimilating information from multiple atmospheric sensing platforms
29 (Hondl 2002).

30

31 The initial prototypes of severe weather information in virtual globes were developed at the
32 National Severe Storms Laboratory (NSSL) and the University of Oklahoma (OU) to support
33 NSSL's mission of enhancing the capability to provide accurate and timely forecasts and
34 warnings of hazardous weather. These prototypes, consisting of data ingest software, severe
35 weather algorithms, weather analysis products and visualization software were developed to
36 assist National Weather Service (NWS) forecasters with warning decision-making for hazardous
37 weather threats such as blizzards, ice storms, flash floods, tornadoes, and lightning. Subjective
38 and objective analyses of the performance of these prototype systems, using virtual globe
39 applications as the primary method to display data to users, have also been carried out (Adrianto
40 *et al.* 2005).

41

42 The original virtual globe for displaying weather data was implemented as part of the Warning
43 Decision Support System – Integrated Information (WDSS-II; Lakshmanan *et al.* 2007). The
44 software, called the WDSS-II Graphics User Interface (GUI; Fig. 1) or “wg”, had the ability to
45 visually blend information from multiple Doppler radars, geostationary weather satellites,
46 lightning detection sensors, in situ observations from surface observing systems, numerical

47 weather prediction models, and many other data sources. In the WDSS-II GUI, users could
48 overlay geographic information in ESRI Shapefile format, query data fields, loop images, and
49 generate cross-sections and isosurfaces of three-dimensional (3D) data fields. The WDSS-II
50 GUI was designed to manage a rapid, large, and continuously updating flow of real-time weather
51 data, and because of this ability it was integrated into operational NWS systems as the Four-
52 dimensional Storm-cell Investigator (Stumpf *et al.* 2006).

53

54 Although the WDSS-II GUI is fairly robust, supported versions were limited to Red Hat Linux-
55 based computers, which exclude a large potential base of end users from utilizing severe weather
56 diagnosis products. In addition, radar data from proximate radars had to be ingested and the
57 severe weather algorithms had to be run locally by NWS forecasters (see Fig. 2). This required
58 hardware, networking and personnel resources that were beyond the capability of many NWS
59 forecast offices.

60

61 With the release of Google Earth and the initial KML specification¹ in 2005 it became possible
62 to generate spatially precise, geo-referenced images for the entire coterminous United States
63 (CONUS) and to distribute these centrally-created products via a web server to a wide audience
64 (Figure 3). This allowed the computationally intensive data processing required to create the
65 severe weather products to be performed centrally. It also permitted accurate, georeferenced
66 display of severe weather information alongside other useful information such as roads, schools
67 and stadia without having to maintain custom software for visualization. Anyone who
68 downloaded Google Earth or other KML-supporting geo-browser would be able to access a

¹KML 2.2 reference

<http://code.google.com/apis/kml/documentation/kmlreference.html>

69 public website² and obtain severe weather information. Prior to becoming early adopters of the
70 KML specification, we had been simply making real-time, automated low-resolution snapshot
71 images of severe weather products in the WDSS-II GUI and posting them on a web site. A
72 combination of high-resolution images and KML files that describe those images enables a much
73 more spatially accurate depiction of the locations of severe weather threats.

74

75 This manuscript describes the data and methods for enabling severe weather threat analysis
76 information inside a KML framework. Section 2 describes several severe weather diagnosis
77 products that are generated by the WDSS-II system. Section 3 explains how these products are
78 translated to KML and image files that can be distributed via the internet. Section 4 illustrates
79 some of the practical applications of these data when they are integrated into a virtual globe
80 display. Several of the strengths and limitations of current virtual globes for use in weather
81 displays are summarized in Section 5.

82

83 **2. Summary of weather products**

84

85 The NSSL and the NWS's Storm Prediction Center cooperatively run an experimental WDSS-II
86 system that generates high-resolution three-dimensional radar reflectivity data and other severe
87 weather guidance products for the continental United States (Lakshmanan *et al.* 2006).

88 Internally, WDSS-II maintains the data it generates in widely used, self-describing and
89 extensible data formats, such as Extensible Markup Language³ (XML) and netcdf.⁴ Some

² WDSS-II experimental real-time weather products
<http://wdssii.nssl.noaa.gov>

³ Extensible Markup Language (XML) 1.0

90 sensors, such as lightning detectors and Doppler radars, provide continuous input data streams,
91 while others, such as satellites or numerical weather prediction models may update only every 15
92 to 60 minutes. The temporal resolution of the various real-time output data sets ranges from 1-
93 minute to hourly updates, while the horizontal spatial resolution is between 0.25 km² and over
94 100 km², depending on the data source (table 1). The vertical resolution of the 3D reflectivity
95 grid from which many products are calculated varies from 0.25 km near the surface to 1 km at 20
96 km Mean Sea Level. The hardware required to generate the real-time products (as of May 2009)
97 includes 45 dual-processor/dual-core servers, each with 16 GB of memory and multiple internal
98 serial-attached SCSI hard disk drives for fast input/output performance. The temporal update
99 rates and latency for the output of continuously streaming input products may be improved via
100 additional processing hardware.

101

102 The products that are generated in the WDSS-II system and translated for viewing in a KML
103 browser are described below.

104

105 (a) Reflectivity

106

107 A single ground-based radar covers a spherical volume of only about 300 km around the radar.
108 Thus, to obtain a 3D grid that covers the entire country, data from more than 140 radars needs to
109 be blended together in real-time [Lakshmanan et. al 2006]. On average, each radar scans a slice
110 of the atmosphere every 15-20 seconds; the central merging system needs to combine the data as

<http://www.w3.org/TR/xml/>

⁴ NetCDF User's Guide for C, An Interface for Data Access, Version 3, April 1997.

<http://www.unidata.ucar.edu/software/netcdf/docs/netcdf/>

111 it arrives and put it into a georeferenced 3D grid. In addition, the radar reflectivity data that is
112 received from the radars does not all consist of precipitation echoes. The echoes could be due to
113 biological returns (such as bats, birds and insects), anomalous propagation (due to atmospheric
114 conditions, the radar beam may be bent downwards and may end up showing buildings and trees
115 rather than clouds) or such artifacts as sun strobos, terrain occultation or instrument errors. Prior
116 to blending reflectivity from the individual radars into a 3D mosaic of data, the reflectivity data
117 are quality controlled to remove non-precipitating echoes (Lakshmanan *et al.* 2007).

118

119 Several radar reflectivity products are generated from the 3D reflectivity field, such as:

- 120 • Lowest Altitude Reflectivity: the reflectivity nearest the ground at each horizontal grid
121 point. This is computed by marching upwards from the surface height and takes into
122 account beam blockage due to mountains and buildings from the location of the radar.
123 Because of beam-blockage, especially in the Mountain West, the lowest altitude
124 reflectivity at a point may be supplied by a radar that is not the closest. This product is
125 used by weather forecasters as an estimate of precipitation reaching the ground;
- 126 • Reflectivity Composite (Fig. 5): the maximum value of reflectivity in the vertical column
127 above each grid point. This is used by weather forecasters to view the full horizontal
128 extent of the storm at all altitudes. High-reflectivity features may be observed in this
129 field that may not appear at the lowest altitude or any one vertical level;
- 130 • Reflectivity at isotherm levels: the reflectivity value at the 0°C, -10°C, and -20°C
131 isotherm, based on the vertical profile of environmental temperature. Hail growth occurs
132 in the vertical layer between 0°C and -20°C, which is usually 3 to 4 km deep. These

133 products provide weather forecasters with a means of identifying intensifying storms that
134 are likely to product hail or lightning in the near future.

135

136 A two-dimensional composite reflectivity field without quality control is also produced for
137 comparison purposes. The un-quality-controlled field is used by many forecasters to identify the
138 location of boundaries where new convection is likely.

139

140 (b) Echo Tops

141

142 The echo top altitude (Fig. 6) is derived from the 3D merged reflectivity grid. At each grid
143 point, this is the highest altitude in the vertical column where the particular reflectivity value is
144 found (18 or 50 dBZ). These products can be useful for quickly identifying rapidly
145 strengthening convection and assessing storm severity. Forecasters use the height of the 50 dBZ
146 echo top as a technique to asses the threat of large hail (Richter *et al.* 2007) The 18 dBZ echo top
147 is used in aviation to determine areas of potentially high turbulence in thunderstorm anvils.

148

149 (c) Relative Echo Heights

150

151 These products, which are very similar to Echo Tops, represent the difference in height between
152 a reflectivity echo top altitude (50 or 30 dBZ) and the altitude of a specific temperature derived
153 from environmental vertical temperature profiles (253K or -20° C; 263K or -10° C; 273K or 0°
154 C). These fields are calculated by subtracting the height of the given isotherm from the echo top
155 in question. Relative Echo Heights are used by forecasters as another method to estimate the

156 severe hail potential in a thunderstorm (Donavon and Jungbluth 2007). These products can be
157 useful for quickly identifying regions where cloud-to-ground lightning may initiate or become
158 more frequent (MacGorman and Rust, 1998).

159

160 (d) Maximum Expected Size of Hail (MESH)

161

162 The MESH product is an estimate of hail size that is based on the vertical profiles of radar
163 reflectivity and environmental temperature (Witt *et al.* 1998; Lakshmanan *et al.* 2006). Because
164 the MESH is calculated for each horizontal grid point, the data show the spatial extent and size
165 distribution of hail cores inside of thunderstorms at a given snapshot in time. Forecasters have
166 made use of the MESH field to provide information to the public via Severe Thunderstorm
167 Warnings about the size of hail to expect. It is also useful as a post-event damage assessment
168 tool when accumulated into a Hail Swath product.

169

170 (e) Hail Swath

171

172 The Hail Swath products (Fig. 6) show the highest observed MESH value for a specific time
173 period, usually 30 minutes or 2 hours, at each grid point. The result is a map of areas that were
174 affected by large hail over that time period. Used in real-time, the Hail Swath shows the past
175 path of the storm and may be used to estimate its direction of movement or to observe changes in
176 direction. Following an event, it may be useful to assess the spatial coverage of potential
177 damage to crops, roofs, and other items that may incur a loss of value when exposed to large
178 hail. Some of the scientific applications of the MESH Hail Swath are discussed in Section 4.

179

180 (f) Vertically Integrated Liquid (VIL)

181

182 The VIL product (Greene and Clark 1972) is a measure of liquid water content in a cloud, and
183 high values have frequently been associated with severe weather. It is calculated by integrating
184 the vertical reflectivity profile above each horizontal grid point and converting it to mass per unit
185 area (kg/m^2). Tall storms with high reflectivity values will result in high VIL values; therefore,
186 VIL is one of several products used by forecasters as a general purpose field to help discriminate
187 between weaker and stronger storms.

188

189 (g) Azimuthal Shear Maximum for 0-2 km and 3-6 km Above Ground Level (AGL)

190

191 Azimuthal shear is calculated using a Linear Least Squares Derivative method (Smith and
192 Elmore 2004) on radial velocity data from individual radars and then blended into a large multi-
193 radar mosaic for the CONUS. The blending process results in a field of maximum positive
194 cyclonic (counter-clockwise in the northern hemisphere) shear. A near-surface (0-2 km AGL)
195 azimuthal shear product highlights circulations and horizontal shear zones in the low altitudes of
196 storms that may be associated with the strong rotation of mesocyclones or tornadic vortex
197 signatures. High values (greater than 0.01 s^{-1}) in the mid-altitude product (3-6 km AGL) may
198 indicate the presence of a deep mesocyclone, indicative of a well-organized supercell
199 thunderstorm that may have a life cycle of up to several hours.

200

201 (h) Rotation Tracks

202

203 The rotation track products (Fig. 7) plot the highest observed Azimuthal Shear Maxima during a
204 specific time interval (usually either 30 minutes or 2 hours). Two sets of rotation tracks are
205 produced at these two time accumulation intervals, the 0-2 km layer rotation track, and the 3-6
206 km mid-altitude layer rotation track. This provides a history of the intensity and spatial coverage
207 of strong storm circulations that may be associated with tornadoes or damaging wind. Some
208 practical applications of the Rotation Tracks products are discussed in Section 4.

209

210 (i) Geostationary Weather Satellite (GOES) data

211

212 Visible, infrared, and water vapor channels are stitched together from GOES-east and GOES-
213 west to make a single image. Forecasters use GOES imagery for a wide variety of purposes,
214 from tracking hurricanes to determining to location of wildfires and observing volcanic ash
215 emissions. In severe storms analysis, the infrared channel is frequently used in conjunction with
216 vertical profiles of environmental temperature to determine the height of to tops of storms and to
217 calculate spatial coverage of cloud cover. The visible channel is used to locate areas where
218 convection is likely to initiate, and to locate “overshooting tops” – cloud tops that are co-located
219 with very strong storm updrafts. Water vapor imagery is useful in assessing the broad
220 distribution of moisture in the atmosphere, and can be used to track large-scale atmospheric
221 waves.

222

223 (j) Lightning Density

224

225 At every 2D grid point, this product provides the density of cloud-to-ground lightning flashes
226 that have been recorded at the grid point in the previous 5 or 15 minutes. The grid is smoothed
227 in a 3x3 neighborhood. The input data used to generate this field may be obtained from one of
228 several lightning strike data feeds that are commercially available. Lightning strikes may occur
229 several km from where the core of a storm is identified with radar data, and therefore this
230 information very useful as a supplementary meteorological data set to assess the intensity and
231 threat area of storm cells.

232

233 (k) Lightning Probability

234

235 At every 2D grid point, this product shows the probability of a cloud-to-ground lightning strike
236 in the next 30 minutes. The algorithm uses current lightning density, a storm motion estimate,
237 satellite data, and radar reflectivity fields as input. The probability is computed using a neural
238 network that was trained on historical data from across the United States (Lakshmanan and
239 Smith 2009). This forecast data field provides guidance for people to go indoors to reduce their
240 exposure to lightning strikes, which kill dozens and injure hundreds of people in the United States
241 each year.⁵

242

243 (l) Surface Observations

244

245 In situ observations from Automated Surface Observing System sites and other surface-based
246 observing systems include measurements of temperature, dew point, pressure, precipitation, wind

⁵ National Weather Service Lightning Safety
<http://www.lightningsafety.noaa.gov/>

247 speed, and wind direction. These observations are among the most-used meteorological data.
248 They are shown on the local television news, kept for the long-term climate record, and ingested
249 into numerical weather prediction model analyses.

250

251 (m) National Weather Service text-based products

252

253 Severe convective weather warnings (tornado, severe thunderstorm, flash flood, and special
254 marine) contain both a text description of the threat and a polygon that outlines the threat area.
255 These products are issued by local NWS forecast offices and typically have duration of 30
256 minutes to a few hours, depending on the warning type. Convective outlooks and convective
257 watches, issued by the Storm Prediction Center, are similar products that cover a larger area at a
258 longer forecast time scale: several hours for a Tornado or Severe Thunderstorm Watch, and one
259 to three days for a Convective Outlook. Local storm reports are point observations of severe
260 weather, usually collected by a storm spotter or from the general public in near-real-time.

261

262 (n) Storm feature tracking

263

264 Storm cell features are identified and tracked using a geospatial image processing technique
265 (Lakshmanan *et al.* 2009; Lakshmanan *et al.* 2003). The algorithm tracks reflectivity features,
266 but also generates statistics based on other input fields so that the trends of those various storm
267 intensity parameters may be displayed. For instance, one may observe how the lightning
268 intensity has changed with a storm cell over time (Fig. 8). Forecasters follow trends of storm

269 parameters to assess whether or not a storm will become severe, or, if it is already severe, to
270 estimate when it will decrease in severity.

271

272 **3. Techniques for visualization**

273

274 The WDSS-II maintains data internally in netcdf and XML formats, but has data conversion
275 routines that are capable of ingesting and writing out data in many different formats. For the
276 purpose of mapping in virtual globes using KML, we focus on only those image formats that are
277 supported by both WDSS-II and KML. The KML NetworkLink tag is used extensively to
278 update the images in real-time. Color scales for the data are available as KML ImageOverlays.
279 All KML GroundOverlay images are time-stamped, and therefore may be animated.

280

281 (a) Two-dimensional data fields

282

283 Two-dimensional data fields are converted into images with supporting KML files using one of
284 three strategies. Image creation relies on the open-source Geospatial Data Abstraction Library⁶
285 (GDAL) or on the open-source Portable Network Graphics⁷ (PNG) library. Two types of image
286 creation simply involve a pixel-to-pixel mapping of a single netcdf file to single GeoTIFF⁸ or
287 PNG files, as WDSS-II also uses a cylindrical (WGS84) coordinate system internally. For each
288 GeoTiff or PNG image, a KML file is generated with a GroundOverlay tag and TimeStamp or

⁶ GDAL - Geospatial Data Abstraction Library

<http://www.gdal.org>

⁷ Portable Network Graphics (PNG) Specification (Second Edition)

<http://www.w3.org/TR/PNG/>

⁸ GeoTIFF

<http://trac.osgeo.org/geotiff/>

289 TimeSpan. GeoTIFF images may be viewed in other Geographic Information System (GIS)
290 software packages that do not support KML, so it may be desirable to generate geoTIFF images
291 in some instances. PNG files have the added benefit of typically being half the size of geoTIFF
292 files, in our implementation, which impacts the bandwidth required to distribute the images.

293

294 Because many of the images generated by WDSS-II may be as large as 20 million pixels in size,
295 a better strategy for generating and distributing them employs the use of the KML Region tags.

296 In this strategy, multiple PNG files (or “tiles”) and supporting KML files are created by WDSS-
297 II and are loaded into the virtual globe based on the level of detail required to match the view.

298 Thus, when viewing from a high elevation in the virtual globe, the full resolution of data is not
299 required because the human eye cannot differentiate that level of detail from a great distance.

300 This greatly increases the processing and bandwidth efficiency of the process, because only the
301 tiles for a specific region and level-of-detail required by the user’s current view are loaded.⁹ In
302 this case, the tiles are created as 256x256 pixel PNG files, and match the Google Maps tile
303 overlay specification.¹⁰

304

305 (b) Polygons

306

307 National Weather Service watches, warning, and outlooks are created with the KML LineString
308 and Polygon tags, and the accompanying text describing the threat is contained in a Placemark
309 tag. Thus, users can see both the area affected and read a detailed description of the weather

⁹ Working with KML Regions

<http://code.google.com/apis/kml/documentation/regions.html>

¹⁰ Google Maps API documentation

<http://code.google.com/apis/maps/documentation/overlays.html>

310 event, overlaid on any of the two-dimensional weather data images and geographic information.

311

312 (c) Point observations

313

314 ASOS observations, storm reports, and storm centroid locations are all displayed via KML

315 Placemark tags. With Google Earth 5 KML extensions, it is possible to embed HTML and

316 Javascript inside a Placemark description, which enables the ability to generate data-driven

317 graphs inside a pop-up balloon (Fig. 8). Our implementation uses the jQuery¹¹ and flot¹²

318 Javascript libraries.

319

320 **4. Severe weather analysis applications of virtual globes**

321

322 Since we started producing and disseminating KML format imagery in 2005, the virtual globe

323 interface to these products has been used extensively to improve the collection of meteorological

324 observations, help validate NWS severe weather warnings, and to monitor severe storms in real-

325 time. Integrating these experimental meteorological data sets with the virtual globe interface via

326 KML and the ability to overlay other geographic data sets such as address and phone number

327 information allows many applications for the data that were not previously possible.

328

329 For example, during the Severe Hazards Analysis and Verification Experiment (SHAVE; Smith

330 *et al.* 2006) real-time 3D CONUS radar data was employed in tandem with geographic

¹¹ jQuery

<http://jquery.com/>

¹² flot

<http://code.google.com/p/flot/>

331 information to create a targeted, high-resolution verification dataset for severe weather. The high
332 temporal and spatial resolution verification data that were collected describes the distribution of
333 hail sizes, wind damage and flash flooding produced by severe thunderstorms. Prior to the initial
334 SHAVE operations in spring 2006, most severe weather reports were collected from storm
335 spotters in the field. The temporal and spatial resolution of these reports was on the scale 30 to
336 60 minutes and over 1000 km² – about the duration and size of a typical NWS Severe
337 Thunderstorm or Tornado Warning. To facilitate research that allows more specific and accurate
338 warnings in the future, a much higher resolution of data is needed – on the order of 10 km² and 1
339 to 5 minutes. Such high-resolution storm damage data sets do not generally exist, except for a
340 few small samples of data collected as part of expensive field projects.

341
342 The SHAVE dataset was collected by scientists who examined MESH, Rotation Track, and flash
343 flood guidance products in a virtual globe, overlaid the data with geo-referenced phone numbers
344 from businesses and residences and used this information to make targeted phone calls. After a
345 storm passed a location, several phone calls were made to these numbers to verify if any severe
346 weather occurred with the storm. This type of data collection has been very effective in creating
347 a much higher temporal and spatial resolution data set of storm reports. Figure 6 shows a
348 comparison of the reports collected by SHAVE and the NWS for a typical event.

349
350 A second way that WDSS-II KML products have been used extensively since 2005 is for
351 guidance in post-event damage surveys. Following a tornado event, damage surveys teams use
352 the Rotation Tracks product to estimate the possible extent of tornado damage and to help plan a
353 route to take to look for tornado damage. In addition to driving routes for NWS, NSSL, and

354 local emergency management survey teams, the Rotation Tracks KML is used to assist the
355 Federal Emergency Management Agency plan routes for aerial surveys of tornado damage, and
356 is used to provide guidance for the International Charter on Space and Major Disasters.
357 Following the completion of an investigation, photographs of damage taken during survey are
358 geo-referenced and may be compared to the high-resolution satellite imagery of Earth's surface
359 contained in virtual globes of what the area of interest looked like before it was damaged.
360 Because of frequent requests for the Rotation Track KML that had expired off of the real-time
361 data stream by survey crews and NWS offices, an automated system was implemented to help
362 fulfill these archived data requests (Manross *et al.* 2008).

363

364 Although these KML severe weather products have not yet become part of the official data
365 streams supported by the NWS for use in forecast offices, many NWS offices do use the data in a
366 virtual globe as part of a situational awareness display during severe weather warning operations
367 (Foster *et al.* 2009). Situational awareness displays, as used by NWS forecasters, are intended
368 to put small-scale thunderstorms into a large-scale perspective, and to provide geographic
369 context for where storms may impact life and property.

370

371 **5. Conclusion**

372

373 Virtual globes are a powerful tool to help users visually integrate meteorological data sets with
374 geographic information to assess impacts of weather events at specific locations. The wide
375 acceptance of the KML standard allows data sets that were previously limited to a purely

376 research-oriented audience to be distributed widely, opening up many new possibilities for the
377 use of these products.

378

379 Stellman *et al.* (2009) describe the use of virtual globes, georeferenced severe weather algorithm
380 products and targeted phone calls to improve the verification efficiency of NWS warnings. They
381 attribute a 10% increase in the rate of Tornado and Severe Thunderstorm Warnings from 2007 to
382 2008 by simply making telephone calls to businesses that they identified as being in the center of
383 the storm's path in Google Earth. Foster *et al.* (2009) describe many ways that virtual globes are
384 used in NWS operations to increase situational awareness during storm events, for impact
385 analysis of events, and severe weather event verification. Our website that serves out
386 georeferenced severe weather products to virtual globe clients was visited by over 10 000 unique
387 visitors in May 2009 alone; over 7 million products were downloaded from the site in just that
388 month.

389

390 The general availability of standard virtual globe clients and the specification of standard data
391 formats and protocols have enabled the democratization of georeferenced data. However, such
392 general purpose tools and software come with the limitation that unique characteristics of
393 weather data sometimes can cause problems. For example, several of the more advanced weather
394 analysis functions in the original WDSS-II GUI, such as the ability to query data, are not yet
395 available in commercially available virtual globes. Instead, images must be interpreted through
396 the use of a color scale to determine approximate data values. There are other shortcomings as
397 well. Because the atmosphere is three-dimensional and rapidly changing in time, future
398 improvements to virtual globes include the need to robustly handle real-time data streams that

399 may have some latency associated. For instance, a satellite image that updates every 15 to 30
400 minutes does not synchronize well in Google Earth with radar data that updates every 2 minutes.

401
402 These limitations can be addressed by building a custom virtual globe client for weather data, but
403 this sacrifices the advantages of a freely available, standardized tool. In practice, therefore, we
404 use a custom virtual globe client (the WDSS-II GUI) for some purposes and the standard virtual
405 globe client (Google Earth and NASA WorldWind) for others. Currently, we are building the
406 WDSS-II GUI functionality on top of the NASA WorldWind Java API so as to derive the
407 benefits of both a standard toolkit and custom functionality.

408

409 **Acknowledgements**

410

411 Funding for this research was provided under NOAA-OU Cooperative Agreement NA17RJ1227.
412 The statements, findings, conclusions, and recommendations are those of the authors and do not
413 necessarily reflect the views of the National Severe Storms Laboratory, the U.S. Department of
414 Commerce, or the University of Oklahoma. The authors thank CIMMS/NSSL scientists (Kurt
415 Hondl, Greg Stumpf, Kevin Manross, Kiel Ortega), the WDSS-II development team (Robert
416 Toomey, Charles Kerr and Jeff Brogden) and NSSL IT staff (Karen Cooper) for their
417 contributions to this project. We also thank all the NWS forecasters and members of the general
418 public who provided feedback and suggestions on the imagery and KML data interface.

References

- Adrianto, I., T. M. Smith, K. A. Scharfenberg, and T. B. Trafalis, 2005: Evaluation of various algorithms and display concepts for weather forecasting. 21st Conference on Interactive Information Processing Systems for Meteorology, Oceanography, and Hydrology, American Meteorological Society, San Diego, CA. 5.7.
- Donavon, R.A., and K.A. Jungbluth, 2007: Evaluation of a technique for radar identification of large hail across the Upper Midwest and Central Plains of the United States. *Weather and Forecasting* 22, 244–254.
- Foster, A., Stellman, K. and Hansing, D., 2009: Using virtual globes to improve situational awareness in the National Weather Service. 25th Conference on International Interactive Information and Processing Systems for Meteorology, Oceanography, and Hydrology, American Meteorological Society, Phoenix, AZ, 13.2.
- Greene, D. R. and R. A. Clark, 1972: Vertically integrated liquid water – A new analysis tool. *Monthly Weather Review* 100, 548–552.
- Hondl, K. D., 2002: Current and planned activities for the Warning Decision Support System – Integrated Information (WDSS-II). Preprints, 21st Conference on Severe Local Storms, American Meteorological Society, San Antonio, TX, 146-148.
- Lakshmanan, V. and T. Smith, 2009: An algorithm to nowcast lightning initiation and cessation in real-time. Fourth Conference on the Meteorological Applications of Lightning Data, American Meteorological Society, Phoenix, AZ, 6.4.
- Lakshmanan, V., K. Hondl, and R. Rabin, An efficient, general-purpose technique for identifying storm cells in geospatial images. *Journal of Oceanic and Atmospheric Technology* 26, 523-37, 2009.
- Lakshmanan, V., A. Fritz, T. Smith, K. Hondl, and G. J. Stumpf, 2007: An automated technique to quality control radar reflectivity data. *Journal of Applied Meteorology* 46, 288-305.
- Lakshmanan, V., T. Smith, G. J. Stumpf, and K. Hondl, 2007: The warning decision support system - integrated information (WDSS-II). *Weather and Forecasting* 22, 592-608.
- Lakshmanan, V., T. Smith, K. Hondl, G. J. Stumpf, and A. Witt, 2006: A real-time, three dimensional, rapidly updating, heterogeneous radar merger technique for reflectivity, velocity and derived products. *Weather and Forecasting*, 21, 802-823.
- Lakshmanan, V., R. Rabin, and V. DeBrunner, 2003: Multiscale storm identification and forecast. *Journal of Atmospheric Research* 67, 367-380.

MacGorman, D.R. and W.D. Rust, 1998: The Electrical Nature of Storms. Oxford University Press, 422 pp.

Manross, K. L., T. M. Smith, J. T. Ferree, and G. J. Stumpf, 2008: An on-demand user interface for requesting multi-radar, multi-sensor time accumulated products to support severe weather verification. 23rd Conference on Interactive Information Processing Systems for Meteorology, Oceanography, and Hydrology, New Orleans, American Meteorological Society, P2.13.

Richter, H., and R.B. Deslandes, 2007: The four large hail assessment techniques in severe thunderstorm warning operations in Australia. Preprints, 33rd Conference on Radar Meteorology, American Meteorological Society, Cairns, Australia, P5.19.

Smith, T.M. and K. L. Elmore, 2004: The use of radial velocity derivatives to diagnose rotation and divergence. Preprints, 11th Conference on Aviation, Range, and Aerospace, American Meteorological Society, Hyannis, MA, P5.6.

Smith, T. M., K. L. Ortega, K. A. Scharfenberg, K.L. Manross, and A. Witt, 2006: The Severe Hail Verification Experiment. Preprints, 23rd Conference on Severe Local Storms, American Meteorological Society, St. Louis, MO, 5.3.

Stellman, K., C. Pieper, K. S. Lander, A. Foster, D. Hansing, and T. Brice, 2009: How enterprise GIS is improving the effectiveness of the National Weather Service. 25th Conference on International Interactive Information and Processing Systems for Meteorology, Oceanography, and Hydrology, American Meteorological Society, Phoenix, AZ, 7A.2.

Stumpf, G. J., M. T. Filiaggi, M. A. Magsig, K. D. Hondl, S. B. Smith, R. Toomey, C. Kerr, 2006: Status on the integration of the NSSL Four-dimensional Stormcell Investigator (FSI) into AWIPS. 23rd Conference on Severe Local Storms, St. Louis, MO, AMS, 8.3.

Witt, A., M. Eilts, G. Stumpf, J. Johnson, E. Mitchell, and K. Thomas, 1998: An enhanced hail detection algorithm for the WSR-88D. Weather and Forecasting, 13, 286–303.

Product	Approx. temporal resolution of output	Approx. spatial resolution of output
Radar reflectivity-based products:	5 min	1 km ²
Reflectivity		
Echo Tops		
Relative Echo Height		
Max Expected Size of Hail		
Vertically Integrated Liquid		
Radar velocity-based products:	2 min	0.25 km ²
Azimuthal Shear		
Rotation Tracks		
Geostationary Weather Satellite:	7-25 min	
Infrared		16 km ²
Visible		1 km ²
Water Vapor		16 km ²
Lightning:	1 min	1 km ²
Density		
Probability		
Surface Observations	15-60 min	Varies
NWS Warnings	1 min	Varies
NWS Storm Reports	1 min	Varies

Table 1: Temporal and spatial resolution of KML products generated by the WDSS-II system in real-time.

Figure Captions

Figure 1: An early version (2000) of the WDSS-II GUI virtual globe with full 3D pan, zoom, tilt, and data interrogation controls and multi-radar data from Arizona.

Figure 2: State of the art circa 2002: In order to utilize multi-radar severe weather algorithms in real-time, a NWS forecast office had to ingest radar data from proximate radars and set up a WDSS-II algorithm server to compute and serve out products on their local area network. These products could then be visualized by a custom-built virtual globe display that provided a georeferenced coordinate system to visualize multiple weather datasets.

Figure 3: In 2005, the availability of a well-supported virtual globe client that could obtain data in standard formats over HTTP using a documented transport protocol enabled us to disseminate highly accurate data that covered the entire coterminous United States (CONUS) over the web. Users of the data required nothing more than a KML browser.

Figure 4: Reflectivity Composite image of Hurricane Wilma (2005) visualized using the Google Earth client and standard data formats and transport protocols.

Figure 5: 18 dBZ echo tops for thunderstorms in Oklahoma visualized using a modified WorldWind client and standard data formats and transport protocols. The ability to overlay geographic data such as roads, cities and schools from other sources is a key advantage of standard virtual globe toolkits. Detailed analysis of data requires the ability to query the raw data values (inset).

Figure 6: 2-hour Hail Swath product overlaid with reports from the Severe Hazards Analysis and Verification Experiment and NWS local storm reports as seen in Google Earth.

Figure 7: 0-2 km Rotation Tracks for the May 3, 1999 tornado outbreak in Central Oklahoma, shown with actual tornado paths from post-event damage surveys (white lines) from the National Oceanic and Atmospheric Administration. The visualization here is using a custom virtual globe built at the National Severe Storms Laboratory.

Figure 8: Reflectivity cluster identification (blue hexagons) with trends of reflectivity (yellow/black) and Lightning Flashes (blue/black). The orange and red polygons are NWS Severe Thunderstorm Warnings and Tornado Warnings, respectively. The visualization here is on Google Earth.

Figure 1
[Click here to download high resolution image](#)



Figure 2
[Click here to download high resolution image](#)

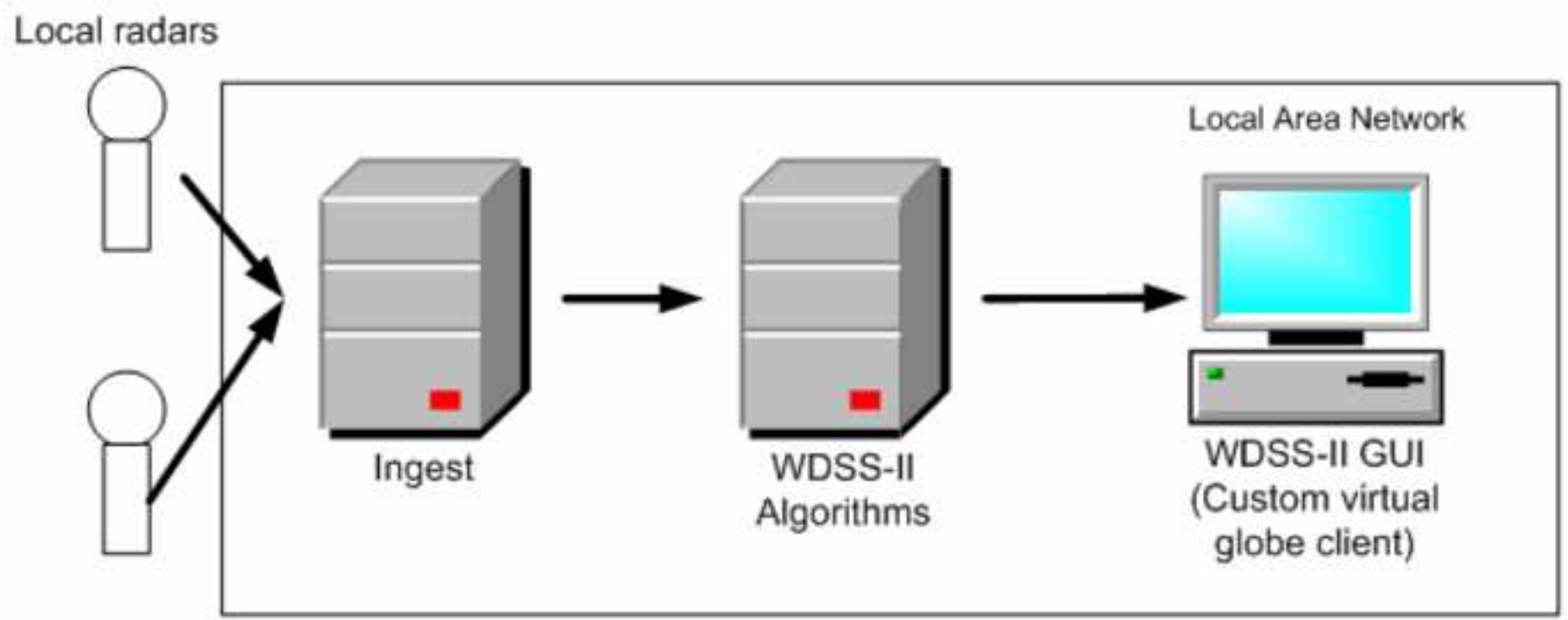


Figure 3
[Click here to download high resolution image](#)

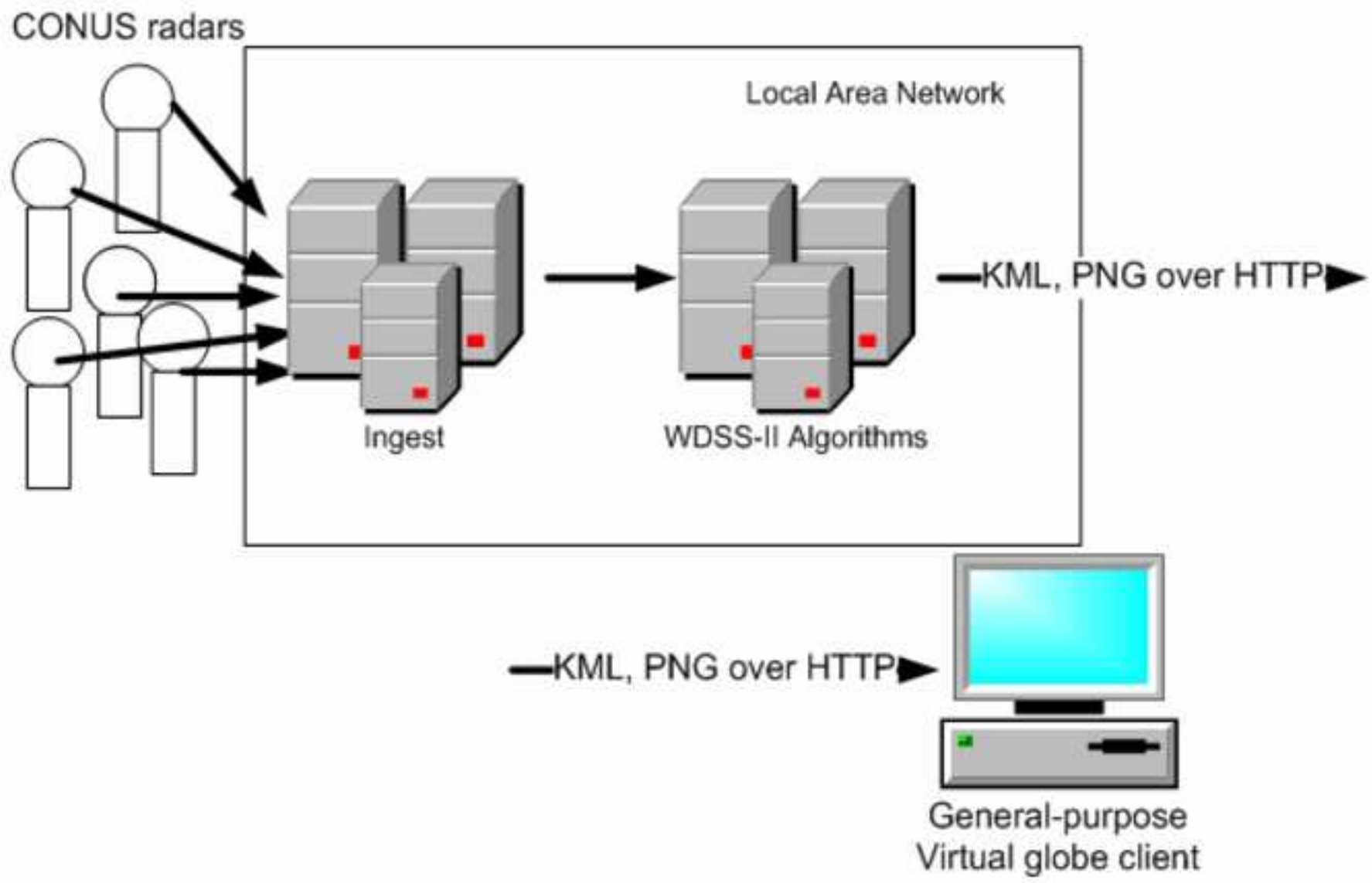


Figure 4
[Click here to download high resolution image](#)

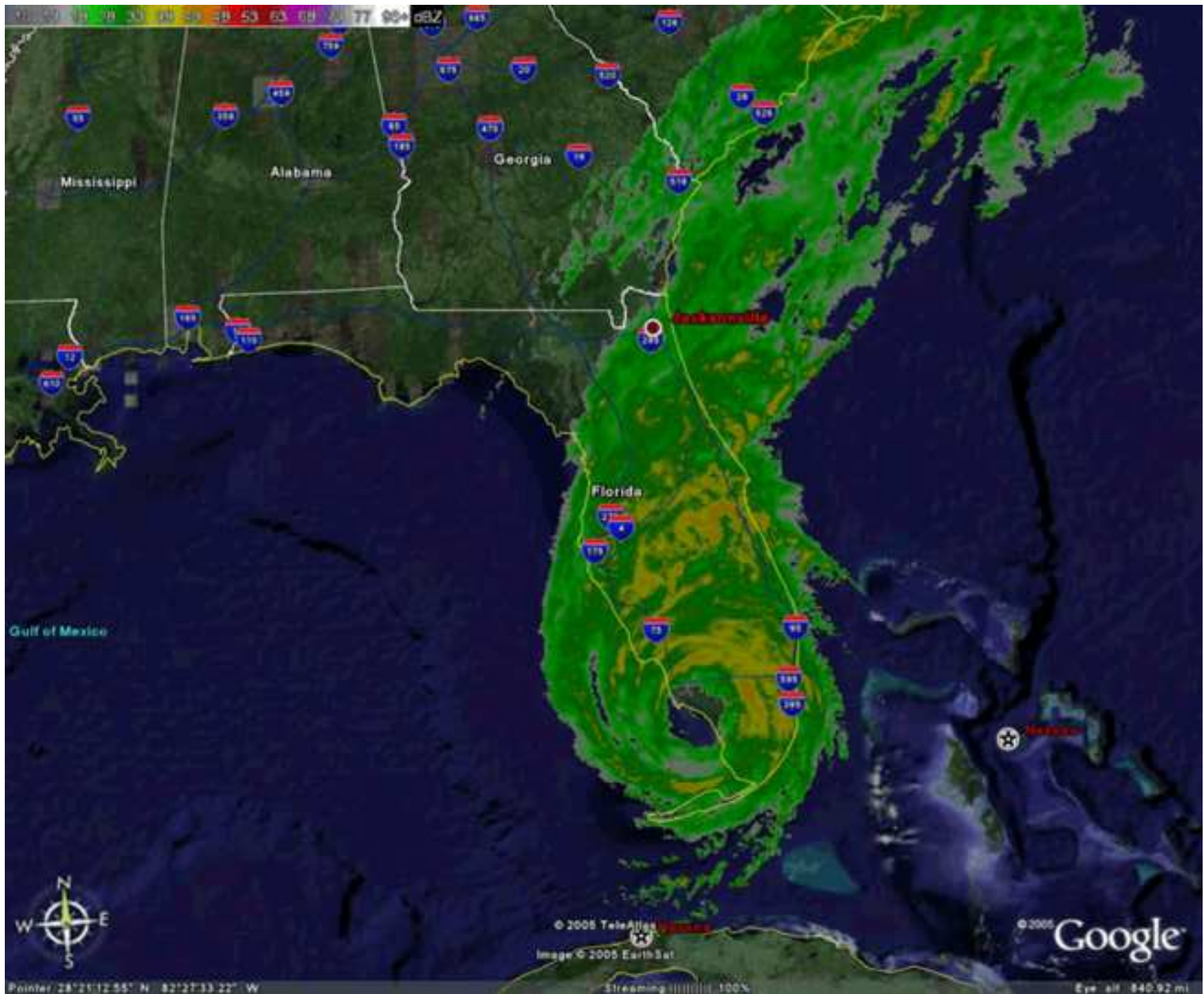


Figure 5
[Click here to download high resolution image](#)

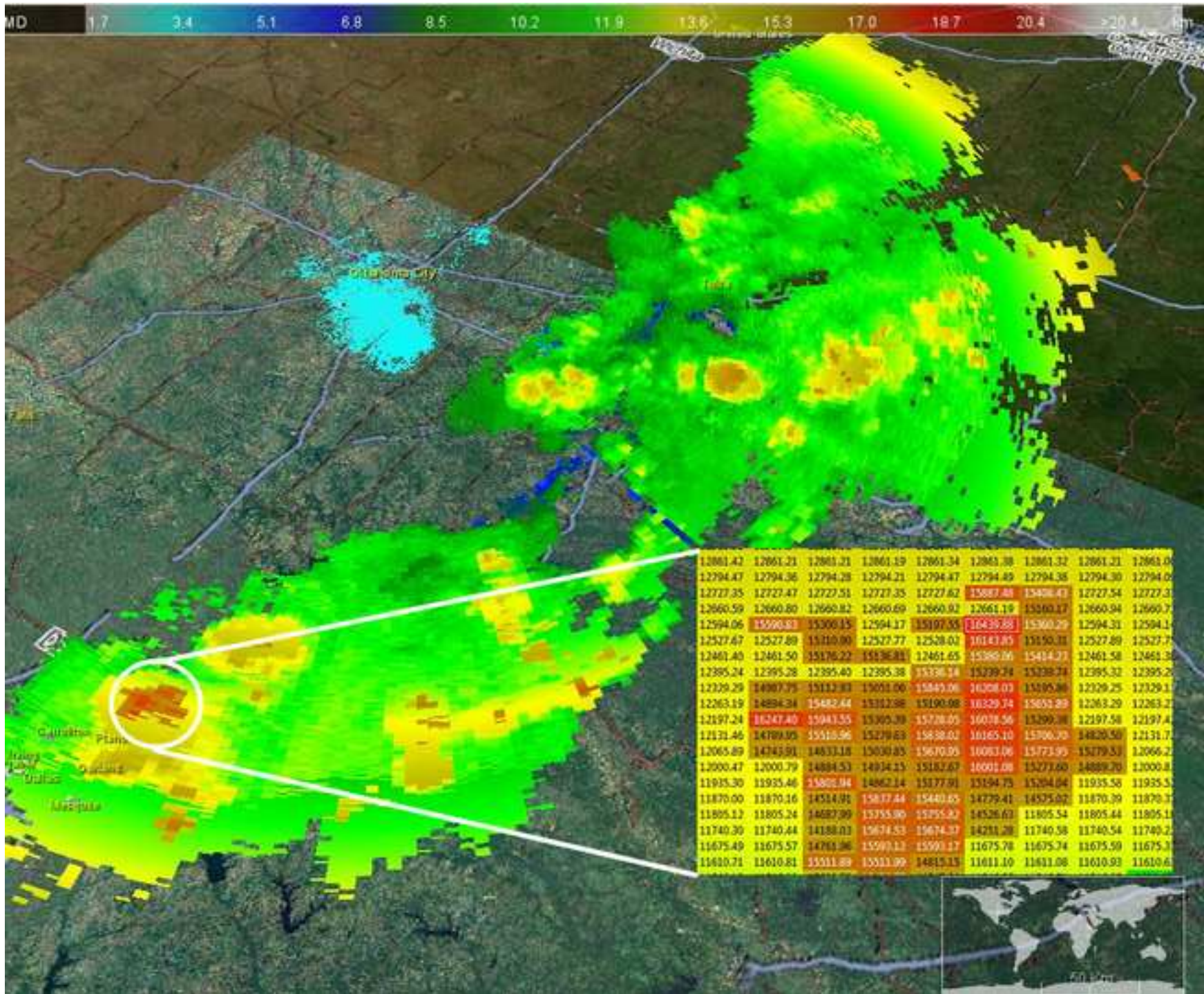


Figure 6
[Click here to download high resolution image](#)

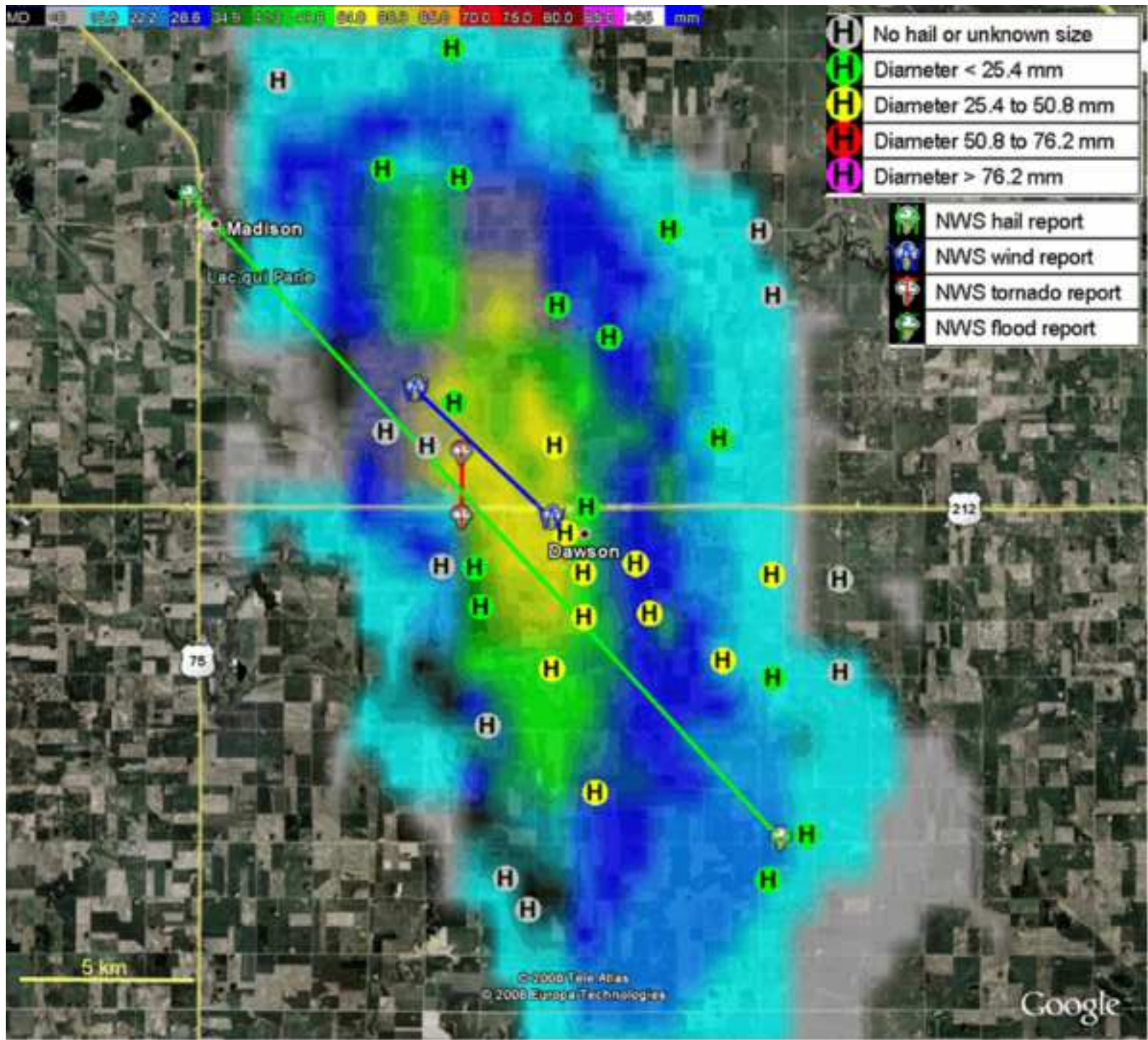


Figure 7
[Click here to download high resolution image](#)

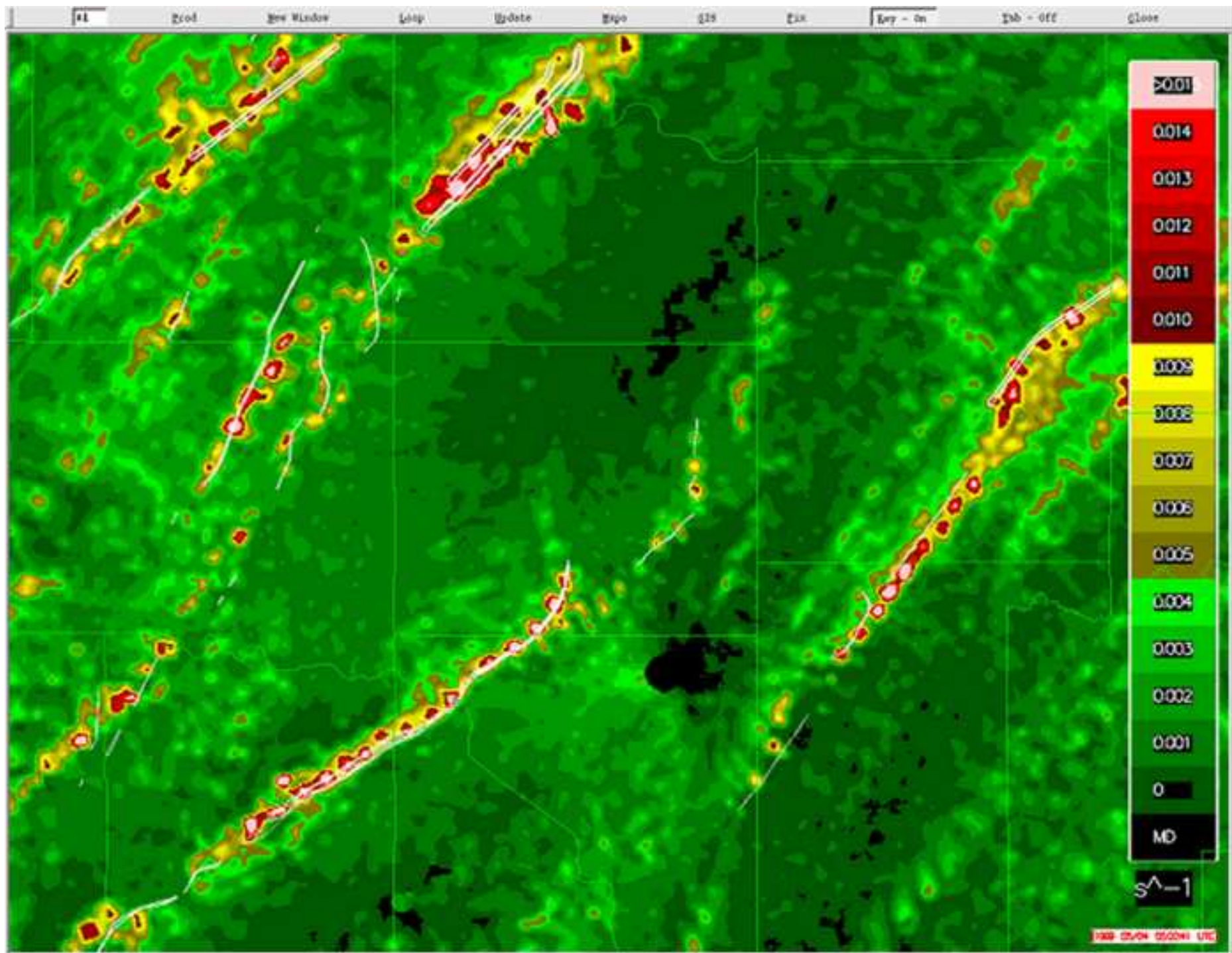


Figure 8
Click here to download high resolution image

